



PERCOLATION THRESHOLD OF POLYMER NANOCOMPOSITES CONTAINING GRAPHITE NANOPATELETS AND CARBON NANOTUBES

Jing LI*, Peng Cheng MA*, Chow Wing SZE*, To Chi KAI*, Ben Zhong TANG**, Jang-Kyo KIM*

*Department of Mechanical Engineering and **Department of Chemistry, Hong Kong University of Science and Technology, Clear Water Bay, Kowloon, Hong Kong

Keywords: *Graphite nanoplatelets, Carbon nanotubes, Nanocomposites, Dispersion, Percolation threshold, Modeling.*

Abstract

An improved analytical model is developed based on an interparticle distance concept, to predict the percolation threshold of conducting polymer composites containing graphite nanoplatelets (GNPs) and carbon nanotubes (CNTs). GNPs are modeled as well-dispersed, disc-shaped cylinders, while CNTs were modeled as either well-dispersed sticks or sphere-shaped CNT agglomerates with a higher CNT concentration than the average CNT content of composites. Two dispersion parameters are introduced in the model to correctly reflect the different dispersion states of CNTs in the matrix. The experimental data collected from literature and previous experiments were compared with the present model, verifying the applicability of the model.

1 Introduction

Conducting polymer composites containing conducting filler and insulating matrix are capable of dissipating electrostatic charges and shielding devices from electromagnetic radiation. Graphite nanoplatelets (GNPs) and carbon nanotubes (CNTs) are nano-scaled conducting fillers with very high aspect ratios. GNPs, consisting of several layers of graphene sheets, are often produced by exfoliating graphite intercalated compound, and are of a thickness range on a nanometer scale with a diameter on a micrometer scale. CNTs, consisting of one or more concentric cylindrical shells of graphene sheets coaxially arranged around a central hollow core, have a diameter on a nanometer scale and length on a micrometer scale. With gradually increasing the conducting filler content, composites

undergo a percolation transition where the electrical conductivity of the composite jumps up several orders of magnitudes and its nature changes from an insulator to a conductor. This behavior is attributed to the formation of conducting network through the insulating matrix material when the filler content is at or above the percolation threshold. The percolation threshold of GNP or CNT reinforced polymer nanocomposites is much lower than the conventional fillers, such as metallic particles, carbon fibres and carbon black, due to their extremely high aspect ratios.

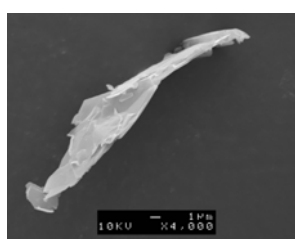
Experimental and theoretical studies have been directed to identify the critical factors that determine the percolation threshold of conducting polymer composites. Based on computational simulations [1], excluded volume approach [2] and renormalization group theory [3], strong correlations were proposed between the percolation threshold and aspect ratio of fillers; the comparison with experiments showed good agreement for composites containing short carbon fibres, microscale disc-shaped graphite flakes and nanoclays with aspect ratios around 100. However, the percolation threshold of CNT/polymer nanocomposites is more complicated than the GNP counterparts. There was no apparent consensus on percolation thresholds of CNT/polymer composites: e.g. the values reported in the literature for typical multiwall CNT/epoxy nanocomposites vary from 0.002 to over 4 wt% [4~12], depending on the type of CNTs and processing techniques used to produce the nanocomposites. The large variation of reported percolation threshold values indicates that the dispersion states and other properties of CNTs affected by different processing conditions are important in determining the electrical properties of the nanocomposite. Theoretical studies have been

made based on similar computational simulation and the excluded volume approach [13,14]. The CNT agglomerates were modeled as close-packed bundle of CNT cylinders forming a cylinder with larger diameters and identical lengths, simplified CNT agglomerates without considering the waviness and 3D entanglement. A two-parametric model was also proposed assuming the CNT agglomerates as spherical inclusions [15] to study the effect of CNT agglomeration on elastic properties of the composite.

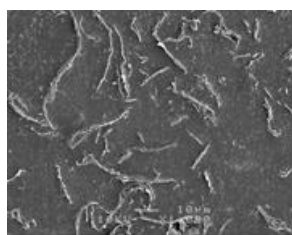
This paper is part of a larger project on the development of conductive polymer composites containing nano-scale fillers, such as GNPs and CNTs. This paper summarizes previous experimental data [16,17,18] and proposes an improved analytical model based on the average interparticle distance (IPD) approach to predict the percolation threshold of polymer nanocomposites. It specifically considers 3D randomly distributed nanoparticles with high aspect ratios [19], as well as the effects of CNT dispersion state [17].

2 Previous experimental results

GNP/epoxy nanocomposites (Figure 1(b)) with good dispersion and high aspect ratio ($\sim 10^4$) of GNP (Figure 1(a)) were fabricated, which gave rise to a very low percolation threshold of 0.5vol% [16,18]. UV/Ozone treatment [16] and bromination treatment [18] did not change the percolation threshold, although it improved the interfacial adhesion. Aspect ratio was found to be a predominant factor on percolation threshold of this composite.



(a)



(b)

Fig. 1. Morphologies of (a) GNP and (b) GNP/epoxy nanocomposites.

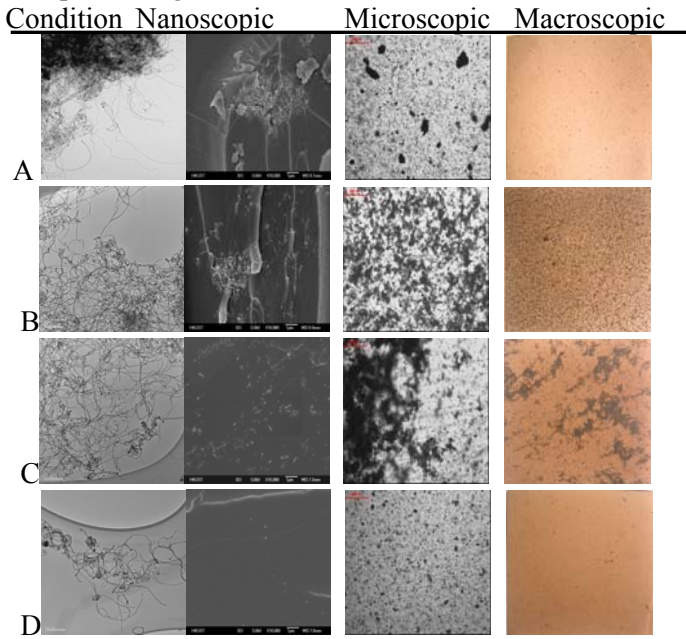
Table 1. Processing methods used to produce nanocomposites and the corresponding percolation thresholds

Condition	Dispersion method	Percolation threshold (vol %)
A	As-received CNTs + epoxy Shear mixing for 30min at 3000rpm	0.26
B	CNTs dispersed by ultrasonication for 1h in acetone+ epoxy ultrasonication for 2h at 60°C	0.06
C	UV/O3 treatment of CNT for 1h and ultrasonication for 2h in acetone + epoxy Shear mixing for 30min at 3000rpm	0.16~0.19
D	CNTs were ball milled for 2 h, ultrasonicated in toluene for 1h UV/O3 treated for 2 h, followed by silane treatment [20], +epoxy ultrasonicated for 2h at 60°C	No percolation

The percolation thresholds of multiwall CNT/epoxy nanocomposites varied from 0.06 vol% to above 0.64 vol% depending on dispersion state and aspect ratio of CNTs produced by different processing conditions (Table 1). The dispersion states of CNTs were characterized on the nano-, micro- and macroscopic scales (Table 2). For CNT/polymer nanocomposites, ‘good dispersion’ has two different meanings: i) ‘disentanglement’ of bundled CNTs or agglomerates, which is ‘nanoscopic dispersion’; and ii) ‘uniform distribution’ of individual CNTs or CNT agglomerates throughout the nanocomposites, which is more of ‘micro- and macroscopic dispersion’. For Condition A, the CNTs were entangled very tightly on a nanoscopic scale and the CNT agglomerates were present in a small localized area on a microscopic scale. The majority of area was unfilled in this composite, so that the composite was transparent on a macroscopic scale. For Condition B, the nanoscopic image indicates that the CNT entanglement was much looser than Condition A due to the ultrasonication process, giving rise to the CNT agglomerates covering a larger area on the micro- and macroscopic scales. Conducting networks were easily formed by these widespread CNT agglomerates, reducing the percolation threshold from 0.26 to 0.06 vol%. For Condition C, although disentanglement of

CNTs was satisfactory on a nanoscopic scale and a large area was covered by CNTs, the corresponding micro- and macroscopic morphologies showed a nonuniform distribution of CNTs. It is thought that the disentangled CNTs, without sufficient surface functional groups, tended to re-agglomerate due to Van der Waals and Coulomb attractions, giving rise to an intermediate percolation threshold of 0.16~0.19 vol%. For Condition D, nanoscopic disentanglement was very satisfactory and CNTs were barely seen on the micro- and macroscopic scales. However, the ball milling and ultrasonication processes used to produce this composite severely reduced the aspect ratio of CNTs. The percolation threshold could not be measured in this case because it was beyond the studied CNT content. In summary, the critical factors determining the percolation threshold of CNT/polymer nanocomposites were identified as i) the aspect ratio of CNTs; ii) disentanglement of CNT agglomerates on the nanoscopic scale; iii) uniform distribution of individual CNTs or CNT agglomerates on the microscopic scale.

Table 2. The dispersion states of CNTs for different processing conditions on different scales.



3 Analyses

An improved analytical model based on the average interparticle distance (IPD) concept is proposed to predict the percolation threshold of

conducting polymer composites containing GNPs and CNTs. The composite is divided into cubic elements with length of L , each containing one conductive particle in the center, and that the total number of cubic elements is equal to the total number of particles [21] :

$$\frac{V_{total}}{L^3} = \frac{V_{filler}}{V_p} \quad (1)$$

where V_{total} is the total volume of composites, V_{filler} is the total volume of filler, V_p is the volume of the individual particle. The conducting fillers are assumed to be homogeneously distributed within the matrix and perfectly bonded with the polymer.

3.1 IPD model for GNP/polymer nanocomposites

For GNP/polymer nanocomposites, GNP was modeled as thin and round platelet with thickness t and diameter D , dispersed individually in the matrix (Figure 2). The volume fraction, P , of GNP is given:

$$P = \frac{V_{filler}}{V_{total}} = \frac{V_p}{L^3} = \frac{\frac{\pi D^2 t}{4}}{[\langle \cos^2 \theta \rangle \cdot (D + IPD)]^3} \quad (2)$$

where IPD is the interparticle distance between adjacent conductive particles; θ represents an angle between the GNP and the direction of preferred orientation; and the angular brackets $\langle \rangle$ denote the orientation average. For a 3D random distribution [22],

$$\langle \cos^2 \theta \rangle = \frac{1}{3} \quad (3)$$

When the IPD is equal to or less than 10nm, electron hopping happens between the adjacent conducting particles, resulting in a rapid increase in electrical conductivity of composite, according to the quantum-mechanical tunneling mechanism [23], and therein filler content P is taken as the percolation threshold P_c . This phenomenon was reported to be independent of the resistivity of the polymer and be applicable to most polymers, organics and oxides. Thus, $IPD = 10$ nm was taken as the criterion for the calculation of percolation thresholds. Combining Eqs. (2) and (3), it gives:

$$P_c = \frac{27\pi D^2 t}{4(D + IPD)^3} \quad (4)$$

As the GNP diameter D is much higher than 10 nm, $D \gg IPD$. Eq. (4) can be reduced to:

$$P_c = \frac{27\pi}{4D} = \frac{21.195}{\alpha} \quad (5)$$

where α is the aspect ratio of GNP, which is identified as the most critical factor for percolation threshold (P_c).

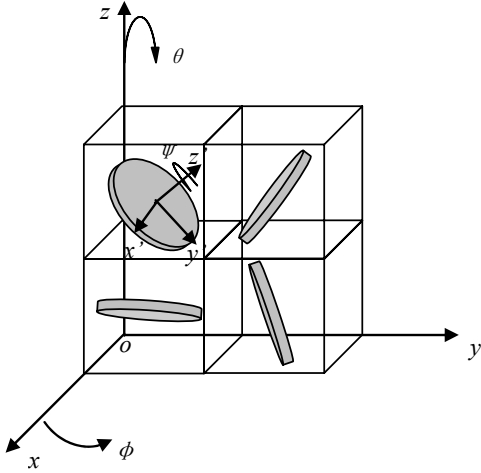


Fig. 2. Schematic drawings of the IPD model for 3D distributed GNP reinforced polymer composites.

3.2 IPD model for CNT/polymer nanocomposites

For CNT/polymer nanocomposites, the conductive particles in the cubic elements could be either a single CNT or a bundle of CNTs, depending on the dispersion state of CNTs:

$$\frac{V_{total}}{L^3} = \frac{V_{filler}}{nV_{CNT}} \quad (6)$$

where V_{CNT} is the volume of the individual CNT, and n is the number of CNTs in an agglomerate (i.e. $n = 1$ in the case of perfect dispersion). To study the effect of the dispersion of CNTs, two extreme cases were considered for the dispersion of CNTs within the polymer matrix: one with all CNTs of cylindrical shape perfectly dispersed in the matrix (Figure 3(a)); and the other with all CNTs present in the form of agglomerates (Figure 3(b)). Suppose that the individual CNT is of a cylindrical shape with length l and diameter d , and the CNT agglomerate exists in the form of a sphere of diameter D' with higher concentration of CNTs than the average filler content. For perfect dispersion where all CNTs are present in the form of individual cylinder, the filler volume fraction is given by the following equation:

$$P = \frac{V_{filler}}{V_{total}} = \frac{V_{CNT}}{L^3} = \frac{\frac{\pi d^2 l}{4}}{[\langle \cos^2 \theta \rangle \cdot (l + IPD)]^3} \quad (7)$$

Similar to the GNP/polymer nanocomposites, $IPD = 10$ nm was taken as the criterion for the calculation of percolation thresholds. As the CNT length l is much longer than 10 nm, $l \gg IPD$. Thus, Eq. (7) is reduced to:

$$P_c \approx \frac{\frac{\pi d^2 l}{4}}{(\frac{1}{3}l)^3} = \frac{27\pi d^2}{4l^2} = \frac{21.195}{\alpha^2} \quad (8)$$

When comparing Eqs. (5) and (8) for two different fillers, it is interesting to note that the geometric shapes of CNT and GNP led to different exponents for the aspect ratio. This observation also indicates that for perfectly-dispersed CNTs and GNPs with similarly high aspect ratios (i.e. identical α value), the CNT composite should have a much lower percolation threshold, P_c , than the GNP counterpart because of the inverse dependency of P_c on α or α^2 .

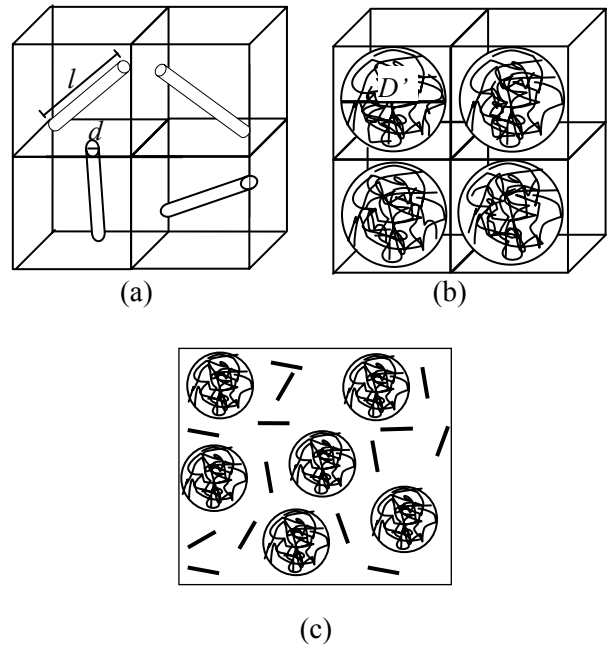


Fig. 3. Models of CNT-reinforced polymer nanocomposites (a) containing perfectly-dispersed CNTs of cylindrical shape, (b) containing CNTs all in the form of agglomerates, and (c) with a mixture of individual CNTs and agglomerates.

On the other hand, if all CNTs are present in the form of agglomerates, P_c is given by:

$$P_c = \frac{V_{filler}}{V_{total}} = \frac{nV_{CNT}}{L^3} \quad (9)$$

To understand how the dispersion state and aspect ratio of CNT affect the percolation threshold of nanocomposites, two descriptive dispersion parameters are introduced: ε , the local volume fraction of CNT in an agglomerate; and ξ , volume fraction of agglomerated CNTs:

$$\varepsilon = \frac{nV_{CNT}}{\frac{\pi D^3}{6}} \quad (P < \varepsilon < 1) \quad (10)$$

$$\xi = \frac{\frac{V_{total}}{L^3} \sum_{i=1}^I n_i V_{CNT}}{V_{filler}} \quad (\text{when } n_i \geq 2) \quad (0 < \xi < 1) \quad (11)$$

A higher ε value corresponds to more tightly entangled CNTs in an agglomerate, and thus the CNT agglomerates cover a smaller volume on a microscopic scale (Table 2). The highest ε value is 1, where CNT agglomerates are closely packed that no polymer matrix is able to penetrate into the agglomerate. Meanwhile, a higher ξ means that the portion of CNTs presents in the form of agglomerates is higher, indicating that a less number of individually-dispersed CNTs exist on the nanoscopic scale (Table 2). The highest ξ value is 1, where all CNTs present in the form of agglomerates. Conversely, in the case of perfect dispersion, no CNT agglomerates exist (at the lowest value of $\xi = 0$) and the localized CNT concentration is the same as the entire nanocomposite (at the lowest value of $\varepsilon = P$). The upper limits, $\varepsilon = 1$ and $\xi = 1$, are undesirable, whereas the lower limits, $\varepsilon = P$ and $\xi = 0$, are favorable to ultra-low percolation threshold of nanocomposites. It should be noted that ε and ξ describe only the ‘degree of CNT entanglement’, which is defined as the ‘nanoscopic dispersion’ in two different ways: i) ε describes how tight the entanglement is and ii) ξ presents how many individual CNTs are entangled in an agglomerate. Non-uniform distribution was not specifically considered in this model, because the overall distribution was assumed to be homogeneous. Incorporating Eq. (10) into Eq. (9) and because $D \gg IPD$ at percolation threshold, we can obtain a simplified equation that depicts the percolation thresholds of nanocomposites with all CNTs in the form of agglomerates:

$$P_c = \frac{nV_{CNT}}{L^3} = \frac{\varepsilon \frac{\pi D^3}{6}}{(D + IPD)^3} \approx \frac{\varepsilon \pi}{6} \quad (12)$$

In practical nanocomposites, however, both the individual perfectly-dispersed CNTs and CNT agglomerates exist (Figure 3(c)). Thus, the percolation threshold of these nanocomposites can be expressed by:

$$P_c = \frac{\xi \varepsilon \pi}{6} + \frac{(1 - \xi) 21.195}{\alpha^2} \quad (13)$$

4 Comparison with Experiments and Discussion

Figure 4 presents the effect of aspect ratio on predicted percolation thresholds of GNP/polymer and CNT/polymer nanocomposites based on Eqs. (5), (8) and (13). Experimental data collected from the literature are superimposed for comparison with the predictions. Table 3 summarizes the materials and processing conditions as well as the corresponding percolation threshold values of the experiments. The predictions are shown as straight lines for perfectly dispersed GNPs (dashed line) and CNTs (solid line), confirming an inverse linear dependence between these parameters on a log scale.

For entangled CNT/polymer nanocomposites, the dispersion parameters, ε and ξ , were assumed to be identical to simplify the calculation of predictions. As expected, the higher the dispersion parameters, the higher the percolation threshold. At low aspect ratios, the percolation threshold decreased in a linear fashion with increasing aspect ratio. As aspect ratio increased further, the percolation threshold presented a gradual transition toward a plateau constant value. The transition occurred over a range of critical aspect ratio, depending on the dispersion parameters. For aspect ratios above the critical range, the percolation threshold became almost constant independent of aspect ratio, and varied only with the dispersion parameters. The existence of this critical range of aspect ratio implies that there are predominant factors that determine the percolation threshold, and the predominant factor changes from aspect ratio to the degree of entanglement with increasing aspect ratio of CNTs. No matter how well the CNTs were disentangled, the percolation threshold could not be lowered below 1 vol% if the aspect ratio was lower than 50.

The comparison with experimental data in Table 3 further verified the applicability of the model. For the experimental results of percolation thresholds reported in wt%, conversion to vol% was made by assuming the densities $\text{GNP} = 2.26\text{g/cm}^3$ and $\text{CNT} = 1.8\text{ g/cm}^3$ [24]. Because of the entanglement of CNTs within the polymer matrix, measuring the CNT lengths with any accuracy was not easy. To approximate the corresponding aspect ratios, three observations reported in the references [9,10,17], including the aspect ratios of as-received CNTs, the processing methods applied and the TEM morphologies, were carefully analyzed. Ultrasonication and ball milling techniques were found to reduce the length of CNTs [25], while magnetic agitation, shear mixing and chemical modification did not.

Table 3 Experimental data used in Figure 4 for various nanocomposites.

Filler	Aspect ratio	Processing method	Pc (vol%)
GNP[26]	600	Two-roll mill	4.46
GNP[27]	1579	Sonication	1.13
GNP[28]	3333	In Situ polymerization	0.878
GNP[29]	4545	Solution blending	0.529
GNP[30]	5000	Solution blending	0.67
GNP[15]	10222	Sonication and shear mixing	0.5
Nonentangled MWNT[4]			
	860	Shear mixing	0.0039
	340	Shear mixing	0.0025
	200	Shear mixing	0.0021
Nonentangled SWNT[12]			
	382	Sonication	0.0052
	152	Sonication	0.0085
Entangled MWNT[9]			
	300	Surfactant and sonication	0.017~0.077
Entangled MWNT[10]			
	1000	Magnetic agitation	0.6
Entangled MWNT[11]			
	417	Magnetic agitation	0.4
	83	Magnetic agitation	1.2
	8	Magnetic agitation	No percolation
Entangled MWNT[17]			
	2000	Condition A	0.26
	500	Condition B	0.06
	200	Condition C	0.19
	<50	Condition D	No percolation

Although there were some experimental discrepancies in the estimation of aspect ratio, the comparisons given in Figure 4 indicate that the prediction in general agreed well with experiments. For GNP/polymer nanocomposites, the coefficient

of determination was 0.903. For non-entangled CNT/polymer nanocomposites [4, 12], the percolation threshold values lie on or slightly below the perfect case predicted by Eq. (8). For entangled CNT/polymer nanocomposites, the comparison between the prediction based on Eq. (13) and the experiments gave the approximate values of the two dispersion parameters, ε and ζ , which were consistent with the dispersion methods applied. The shear mixing (Condition A) helped little with disentanglement of CNT agglomerates, so that the corresponding dispersion parameters ranged from 0.05 to 0.1. For Condition B, ultrasonication resulted in disentanglement of CNT agglomerates to a certain extent, while reducing the aspect ratio, which in turn decreased the percolation threshold with the dispersion parameters ranging between 0.01 and 0.05. For Condition C, although the disentanglement was quite satisfactory, both the dispersion parameters were about 0.05 because of the non-uniform distribution of CNTs. The experimental data taken from the literature were also analyzed similarly based on the processing information. When CNTs were processed by mild oxidation, surfactant, ultrasonication and two-roll milling [9], the nanoscopic dispersion was good as proven by the TEM and SEM photographs. Thus, the near perfect dispersion state was reflected in Figure 4. For the CNTs dispersed in methanol by magnetic stirring [10, 11], the percolation thresholds were relatively high due to the inadequate disentanglement of CNT agglomerates with both the dispersion parameters approximately 0.1. The arrows in Figure 4 represent the results for Condition D from Ref. [17] and [11], where the aspect ratios of the CNTs were too low to show obvious percolation for the CNT contents employed.

The above explanations together with the previous experimental studies summarized in Table 3 confirmed the applicability of the present model to establish the correlations between the percolation thresholds, the aspect ratio and the degree of CNT disentanglement in CNT/polymer and GNP/polymer nanocomposites. Nevertheless, there are a few parameters that cannot be taken into account in the present IPD model. They include 1) irregular shape of GNPs, different from the perfect cylindrical shape assumed in the model; and 2) agglomeration of GNPs and microscopic nonuniform distribution of CNTs, different from the assumption of homogeneous overall distribution made in the model; and 3) presence of micro-flaws or debonding between the matrix and particles, different from the

assumption of perfect bonding. These parameters as well as the errors in estimating filler aspect ratios may be responsible for the discrepancies between the prediction and experimental data.

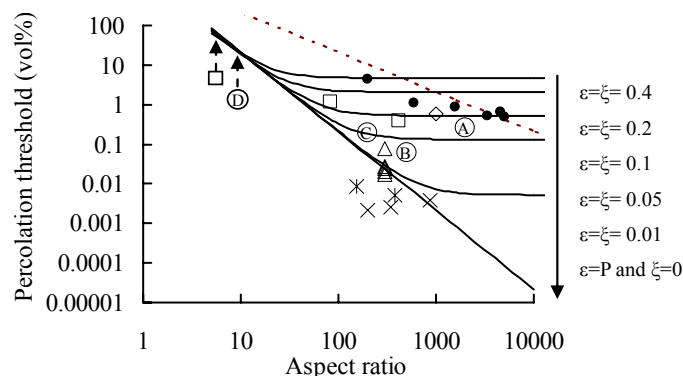


Fig. 4. Effects of aspect ratio on percolation threshold of polymer nanocomposites containing GNP (dashed line) or CNT (solid lines). Experimental data: GNP/polymer nanocomposites • [18]; CNT/polymer nanocomposites fabricated by Conditions A, B, C and D ○ [17]; △ [9]; ◇ [10]; □ [11]; * [12].

5 Conclusions

An improved model was proposed based on the average interparticle distance concept to predict the percolation threshold of CNT or GNP-reinforced polymer nanocomposites. Two descriptive dispersion parameters were introduced to take the dispersion state of CNTs into consideration. Major findings are highlighted as follows:

1. The model formulated in this study can be used to establish the correlations between the percolation threshold, dispersion state and aspect ratio of CNTs and GNPs.

2. For perfectly dispersed CNTs or GNPs, the aspect ratio was found to be the predominant factor determining the percolation threshold.

3. For entangled CNT/polymer nanocomposites, there was a critical value of CNT aspect ratio, above which the two dispersion parameters became crucial allowing the percolation threshold to vary several orders of magnitude, while below it the percolation threshold increased rapidly with decreasing aspect ratio.

4. The present IPD model agreed well with experimental data collected from the literature, confirming its applicability to predict the percolation behaviors of nanocomposites.

References

- [1] Balberg I., Binenbaum N. and Wagner N. "Percolation thresholds in the three-dimensional sticks system". *Phys. Rev. Lett.*, Vol. 52, No.17, pp 1465–1468, 1984.
- [2] Celzard A., McRae E., Deleuze C., Dufort M., Furdin G. and Mareche JF. "Critical concentration in Percolating systems containing a high-aspect-ratio filler". *Phys. Rev. B*, Vol. 53, No. 10, pp 6209–6214, 1996.
- [3] Lu C. and Mai Y. W. "Influence of aspect ratio on barrier properties of polymer-clay nanocomposites". *Phys. Rev. Lett.*, Vol. 95, pp 088303-1–088303-4, 2005.
- [4] Martin C. A., Sandler J. K. W., Shaffer M. S. P., Schwarz M. K., Bauhofer W., Schulte K. and Windle A. H. "Formation of percolating networks in multi-wall carbon-nanotube-epoxy composites". *Compos. Sci. Tech.*, Vol. 64, pp 2309-2316, 2004.
- [5] Martin C. A., Sandler J. K. W., Windle A. H., Schwarz M. K., Bauhofer W., Schulte K. and Shaffer M. S. P. "Electric field-induced aligned multi-wall carbon nanotube networks in epoxy composites". *Polym.*, Vol. 46, pp 877-886, 2005.
- [6] Sandler J. K. W., Kirk J. E., Kinloch I. A., Shaffer M. S. P. and Windle A. H. "Ultra-low electrical percolation threshold in carbon-nanotube-epoxy composites". *Polym.*, Vol. 44, pp 5893-5899, 2003.
- [7] Moiala A., Li Q., Kinloch I. A. and Windle A. H., "Thermal and electrical conductivity of single- and multi-walled carbon nanotube-epoxy composites". *Compos. Sci. Tech.*, Vol. 66, pp 1285-1288, 2006.
- [8] Gojny F. H., Wichmann M. H. G., Fiedler B., Kinloch I. A., Bauhofer W., Windle A. H., Schulte K. *Polym.*, Vol. 47, pp 2036-2045, 2006.
- [9] Kim Y. J., Shin T. S., Choi H. D., Kwon J. H., Chung Y. C. and Yoon H. G. "Electrical conductivity of chemically modified multiwalled carbon nanotube/epoxy composites." *Carbon*, Vol. 43, pp 23-30, 2005.
- [10] Allaoui A., Bai S., Cheng H. M. and Bai J. B. "Mechanical and electrical properties of a MWNT/epoxy composite". *Compos. Sci. Tech.*, Vol. 62, pp 1993-1998, 2002.
- [11] Bai J. B. and Allaoui A. "Effect of the length and the aggregate size of MWNTs on the improvement efficiency of the mechanical and electrical properties of nanocomposites—

- experimental investigation". *Compos.: Part A*, Vol. 34, pp 689-694, 2003.
- [12] Foygel M., Morris R. D., Anez D., French S. and Sobolev V. L. "Theoretical and computational studies of carbon nanotube composites and suspensions: Electrical and thermal conductivity." *Phys. Rev. B*, Vol. 71, pp 104201-1–104201-8, 2005.
- [13] Bryning M. B., Islam M. F., Kikkawa J. M. and Yodh A. G. "Very low conductivity threshold in bulk isotropic single-walled carbon nanotube-epoxy composites". *Adv. Mater.*, Vol. 17, pp 1186-1191, 2005.
- [14] Grujicic M., Cao G. and Roy W. N. "A computational analysis of the percolation threshold and the electrical conductivity of carbon nanotubes filled polymeric materials". *J. Mater. Sci.*, Vol. 39, pp 4441-4449, 2004.
- [15] Shi D. L., Feng X. Q., Huang Y. Y., Hwang K. C. and Gao H. "The Effect of Nanotube Waviness and Agglomeration on the Elastic Property of Carbon Nanotube-Reinforced Composites". *J. Eng. Mater. Technol.*, Vol. 126, pp 250-257, 2004.
- [16] Li J., Sham M. L., Kim J. K. and Marom G. "Morphology and properties of UV/Ozone treated graphite nanoplatelet/epoxy nanocomposites". *Compos. Sci. Tech.*, Vol. 67, pp 296–305, 2006.
- [17] Li J., Ma P. C., Sze C. W., Kai T. C., Tang B. Z. and Kim J. K. "Correlations between percolation threshold, dispersion state and aspect ratio of carbon nanotubes." *Advanced Functional Materials*, 2007 accepted.
- [18] Li J., Vaisman L., Marom G. and Kim J. K. "Br treated graphite nanoplatelets for improved electrical conductivity of polymer composites". *Carbon*, Vol. 45, pp 744–750, 2007.
- [19] Li J. and Kim J. K. "Percolation Threshold of conducting polymer composites containing 3D randomly distributed graphite nanoplatelets". *Compos. Sci. Tech.*, 2007, in press.
- [20] Ma P.C., Kim J.K. and Tang B.Z. "Functionalization of Carbon Nanotubes Using A Silane Coupling Agent". *Carbon*, Vol. 44, pp 3232-3238, 2006.
- [21] El-Tantawy F. and Deghaidy F. S. "Effect of iron oxide on vulcanization kinetics and electrical conductance of butyl rubber composites". *Polym Int*, Vol. 49, pp 1371–1376, 2000.
- [22] Chandrasekhar S. "*Liquid crystals*", Cambridge University Press, New York, 1992.
- [23] Fiuschau G. R., Yoshikawa S. and Newnham R. E. "Resistivities of conductive composites". *J. Appl. Phys.*, Vol. 72, pp 953-959, 1992.
- [24] Xie X. L., Mai Y. W. and Zhou X. P. "Dispersion and alignment of carbon nanotubes in polymer matrix: A review". *Mater. Sci. Eng. R*, Vol. 49, pp 89-112, 2005.
- [25] Hilding J., Grulke E. A., Zhang Z. G. and Lockwood F. "Dispersion of carbon nanotubes in liquids". *J. Disper. Sci. Technol.*, Vol 24, pp 1-41, 2003.
- [26] Weng W. G., Chen G. H., Wu D. J. and Yan W. L. "HDPE/expanded graphite electrically conducting composite". *Compos. Interface*, Vol. 11, No. 2, pp 131–143, 2004.
- [27] Fukushima H. and Drzal L. T. "Graphite nanocomposites: structural and electrical properties." *Proc. 14th Int. Conf. Compos. Mater. (ICCM-14)*, San Diego, July 2003.
- [28] Chen G. H., Wu D. J., Weng W. G. and Yan W. L. "Preparation of polymer/graphite conducting nanocomposite by intercalation polymerization". *J. Appl. Polym. Sci.*, Vol. 82, pp 2506-2513, 2001;
- [29] Zheng W. and Wong S. C. "Electrical conductivity and dielectric properties of PMMA/expanded graphite composites". *Compos. Sci. Technol.*, Vol. 63, pp 225-235, 2003.
- [30] Chen X. M., Shen J. W. and Huang W. Y. "Novel electrically conductive polypropylene/graphite nanocomposites". *J. Mater. Sci. Lett.*, Vol. 21, pp 213–214, 2002.